NASA TN D-1441

TECHNICAL NOTE

D-1441

COMBINED RADIATION AND FORCED CONVECTION FOR FLOW OF A TRANSPARENT GAS IN A TUBE WITH SINUSOIDAL AXIAL WALL HEAT FLUX DISTRIBUTION

By Robert Siegel

Lewis Research Center
Cleveland, Ohio

NATIONAL AERONAUTICS AND SPACE ADMINISTRATION

WASHINGTON October 1962

NATIONAL AERONAUTICS AND SPACE ADMINISTRATION

TECHNICAL NOTE D-1441

COMBINED RADIATION AND FORCED CONVECTION FOR FLOW OF A TRANSPARENT GAS IN A TUBE WITH SINUSOIDAL AXIAL WALL HEAT FLUX DISTRIBUTION

By Robert Siegel

SUMMARY

An analysis is made of the influence that radiation exchanges between elements on the inside surface of a tube have on the wall and gas temperature distributions for forced-convection flow. The wall heat generation has a chopped sine distribution with length along the tube, which is a distribution often encountered in nuclear-reactor channels. The flowing gas is assumed transparent to thermal radiation and hence does not participate directly in the radiative exchange process. Axial heat conduction is neglected in the gas and tube wall, and the convective-heat-transfer coefficient and fluid properties are assumed constant. Several numerical examples are given to illustrate the effects of eight independent parameters such as wall emissivity, Stanton number, and length-diameter ratio. In some instances the radiation exchanges reduced the peak wall temperature or caused a reduction in the exit gas temperature because of radiation losses from the tube end openings.

INTRODUCTION

In advanced types of powerplants it is desirable to increase the operating temperature levels to achieve higher efficiencies. With higher surface temperatures, heat exchange by radiation is more significant and can become coupled with conduction and convection processes. This report is concerned with combined radiative and convective heat transfer for flow of a transparent gas in a tube.

The first interest in this situation was shown by Hottel (ref. 1), who derived the energy balances for combined radiation and convection in a uniformly heated black tube. The energy balance on an element of the tube wall resulted in a nonlinear integral equation, while the gas temperature was governed by a first-order linear differential equation.

In reference 1, one numerical solution was obtained for a short tube by dividing the tube length into several isothermal zones and writing a heat balance for each region. This gave a set of nonlinear equations that were solved for an average temperature in each zone. This analysis was continued in reference 2 where the governing integral equation was transformed into a differential equation by using an approximate separable kernel. Numerical examples were then carried out to examine in detail the influence of the several independent parameters. In reference 3 a uniformly heated gray tube was analyzed by using the net radiation method (ref. 4, pp. 21-24) combined with the procedures utilized in reference 2.

The present report extends the previous analyses to include arbitrary variations in wall heat flux along the tube length. The analysis is carried out for an arbitrary axial heat flux variation and is then specialized for a chopped sinusoidal distribution that is often encountered in nuclear-reactor passages. The gas flowing in the tube is assumed transparent to radiation so that radiant exchanges occur only between elements of the internal tube surface that are at different temperatures, and between the internal tube surface and the environment outside each end of the tube. When internal radiation exchanges within the tube are appreciable, the local heat convection to the gas is no longer equal to the local heat generation supplied to the wall but is equal to this heating plus the net radiative gain. Throughout the analysis the convective-heat-transfer coefficient between the wall and gas is assumed constant, and this assumption will be discussed later. The outside surface of the tube is assumed perfectly insulated and, hence, has no heat exchange from it. The equivalent of this condition can occur when the flow channel is surrounded by other channels that are similarly heated. For example, in a reactor fuel element constructed of an array of stacked parallel plates with flow between them, half the energy from each plate is transferred into the channel on each side. From symmetry, the temperature derivative is zero at the center of each plate thickness, which corresponds to an insulated boundary condition.

In the next section the energy equations will be derived for an arbitrary variation in wall heating with axial position. The equations will then be reduced to a set of two simultaneous differential equations that can be solved by standard numerical forward integration methods.

ANALYSIS

The circular tube under consideration is shown in figure 1. The heat imposed at or generated in the tube wall is supplied either by some external means such as electrical heating or by nuclear fission of fuel contained in the wall. The heat input can vary in an arbitrary manner

along the tube length and is given by $q(X)$. The integrated average heat addition is given by the definition

$$\overline{q} = \frac{1}{L} \int_0^L q(X)dX \tag{1}$$

Each end of the tube is exposed to a reservoir or outside environment that is maintained at a given temperature. At the inlet end of the tube this temperature is $T_{r,i}$, and at the exit it is $T_{r,e}$. The gas flowing through the tube enters at temperature $T_{g,i}$ and leaves at $T_{g,e}$. The gas is assumed transparent to thermal radiation so that it does not participate directly in the radiative exchange. This is a reasonable assumption for gases such as hydrogen, oxygen, and nitrogen. This assumption is also valid for radiating gases when the densities and path lengths (i.e., optical thicknesses) are small so that the gaseous radiation is small compared with the radiative exchanges between the solid boundaries. The inside surface of the tube wall is assumed to be diffuse and gray so that the emissivity ϵ is independent of wavelength and is equal to the absorptivity. In addition, ϵ is assumed independent of temperature so that it is constant throughout the tube. As will be shown later, for long tubes the results are generally insensitive to the value of ϵ, so this is not a very restricting assumption. The convective-heat-transfer coefficient between the wall and gas is assumed constant throughout the tube. This causes an error in the thermal entrance length where the heat-transfer coefficient is higher than in the fully developed region. For turbulent flow the thermal entrance lengths for gases are fairly short, on the order of 10 diameters, so this assumption becomes less important when long tubes on the order of 50 to 100 diameters are under consideration. The variation of heat flux along the tube length also has an influence on the heat-transfer coefficient, but is a relatively minor effect for turbulent conditions.

Energy Balance

The energy balance is derived in the same manner as in reference 3 where a uniformly heated gray tube was considered. According to Poljak's net radiation method (ref. 4), q_o and q_i are the rates of outgoing and incoming energy for the surface resulting only from the radiative processes. At any location along the tube wall the energy supplied to the wall is $q + q_i$, where q is the specified external heat addition or heat generation in the tube wall. The energy leaving the wall because of radiation and convection is $q_o + h(T_w - T_g)$. This gives the heat balance

$$q(x) + q_i(x) = q_o(x) + h\left[T_w(x) - T_g(x)\right] \tag{2}$$

where the coordinate x has been nondimensionalized in terms of the tube diameter. The outside surface of the tube is assumed perfectly insulated and hence does not provide any additional terms in the heat balance.

Expressions for q_i and q_o are needed so that these quantities can be eliminated in terms of the desired wall and gas temperatures. The incoming radiation q_i at a given x location is composed of radiation coming from surface elements at other positions ξ along the tube and from the reservoirs at the inlet and exit ends. This gives the relation

$$q_i = \int_0^l q_o(\xi)K(|x - \xi|)d\xi + \sigma T_{r,i}^4 F(x) + \sigma T_{r,e}^4 F(l - x) \tag{3}$$

The integral is the energy contribution that the outgoing radiation $q_o(\xi)$ from all the other surface elements makes to the element at x. The q_o at ξ has to be multiplied by the geometrical configuration factor $K(|x - \xi|)d\xi$ to give the amount of radiant energy leaving a ring area element at ξ that reaches x. This factor is given by

$$K(|x - \xi|)d\xi = \left\{1 - \frac{|x - \xi|^3 + \frac{3}{2}|x - \xi|}{\left[(x - \xi)^2 + 1\right]^{3/2}}\right\}d\xi \tag{4}$$

The two other terms on the right side of equation (3) are the heat loads coming from the inlet and outlet environments at the ends of the tube. Each environment is represented by a black plane at the end of the tube that assumes the radiation coming through each end opening is diffusely and uniformly distributed over the end opening. The quantity F is the geometrical configuration factor between a ring element of differential length on the tube wall and the circular opening at the end of the tube; F is based on the area of the element on the tube wall and is given by

$$F(x) = \frac{x^2 + \frac{1}{2}}{(x^2 + 1)^{1/2}} - x \qquad x \geq 0 \tag{5}$$

In equation (2) the outgoing radiation q_o from a surface is made up of directly emitted radiation plus the amount of incoming radiation that is reflected:

$$q_o = \epsilon\sigma T_w^4 + \rho q_i \tag{6}$$

Since the surface is opaque, the reflectivity ρ is equal to one minus the absorptivity, which, with the gray assumption, becomes $1 - \epsilon$. Then

$$q_o = \epsilon\sigma T_w^4 + (1 - \epsilon)q_i \tag{6a}$$

Since the three equations (eqs. (2), (3), and (6a)) contain four unknowns - q_o, q_i, T_w, and T_g, an additional relation is required. This is found from a heat balance on the flowing gas. The gas is assumed transparent to thermal radiation so it exchanges heat with the wall only by convection. If a cylindrical control volume in the gas of diameter D and differential length dX is considered, the convected energy flowing into the volume is $\frac{\pi D^2}{4}\,\overline{u}\rho c_p T_g$, while that convected out is

$$\frac{\pi D^2}{4}\,\overline{u}\rho c_p T_g + \frac{d}{dX}\left(\frac{\pi D^2}{4}\,\overline{u}\rho c_p T_g\right)dX$$

The energy convected to the gas from the wall is $\pi D\, dX\, h(T_w - T_g)$. The energy balance on the gas is then

$$\frac{dT_g}{dx} = St(T_w - T_g) \tag{7}$$

where $x = X/D$ and St is the Stanton number $4h/\overline{u}\rho c_p$.

Since equations (2), (3), (6a), and (7) are to be solved for T_w and T_g, q_i, which is not of physical interest, must be eliminated first. Substituting equation (3) into (2) gives

$$q(x) + \int_0^l q_o(\xi)K(|x - \xi|)d\xi + \sigma T_{r,i}^4 F(x) + \sigma T_{r,e}^4 F(l - x)$$

$$= q_o(x) + h\left[T_w(x) - T_g(x)\right] \tag{8}$$

Equations (2) and (6a) can also be combined to eliminate q_i:

$$q_o = \sigma T_w^4 + \frac{1 - \epsilon}{\epsilon}\left[h(T_w - T_g) - q(x)\right] \tag{9}$$

Equations (7), (8), and (9) then constitute a set of three equations for three unknowns - q_o, T_w, and T_g. Before proceeding with the solution,

the equations are placed in dimensionless form:

$$\frac{dt_g}{dx} = St\left[t_w(x) - t_g(x)\right] \tag{7a}$$

$$\frac{q(x)}{\bar{q}} + \int_0^l \frac{q_o}{\bar{q}}(\xi)K(|x - \xi|)d\xi + t_{r,i}^4 F(x) + t_{r,e}^4 F(l - x)$$

$$= \frac{q_o(x)}{\bar{q}} + H\left[t_w(x) - t_g(x)\right] \tag{8a}$$

$$\frac{q_o}{\bar{q}} = t_w^4 + \frac{1 - \epsilon}{\epsilon}\left[H(t_w - t_g) - \frac{q(x)}{\bar{q}}\right] \tag{9a}$$

Separable Kernel Approximation

The integral equation (8a) is complicated by the fact that the kernel $K(|x - \xi|)$ is not a simple algebraic function. It is shown in references 5 and 6 that a good approximation for K is

$$\left.\begin{aligned} K(x - \xi) &\cong e^{-2(x-\xi)} \qquad x > \xi \\ K(\xi - x) &\cong e^{-2(\xi-x)} \qquad x < \xi \end{aligned}\right\} \tag{10}$$

The use of this exponential approximation provides a great simplification since $e^{-2(x-\xi)} = e^{-2x}e^{2\xi}$ is a separable function, that is, a product of a function of x alone and a function of ξ alone. This approximation is introduced into equation (8a) to give

$$\frac{q(x)}{\bar{q}} + \frac{1}{e^{2x}}\int_0^x \frac{q_o(\xi)}{\bar{q}} e^{2\xi}\, d\xi + e^{2x}\int_x^l \frac{q_o(\xi)}{\bar{q}} e^{-2\xi}\, d\xi$$

$$+ t_{r,i}^4 F(x) + t_{r,e}^4 F(l - x) = \frac{q_o(x)}{\bar{q}} + H\left[t_w(x) - t_g(x)\right] \tag{11}$$

Hence, by using equation (10) the x function in K can be taken out from under the integral signs.

Reduction to differential equation. - Equation (11) can now be simplified by transforming it into a differential equation. It is first differentiated twice to give

$$\frac{1}{\overline{q}}\frac{d^2q}{dx^2} + \frac{4}{e^{2x}}\int_0^x \frac{q_o(\xi)}{\overline{q}} e^{2\xi}\, d\xi + 4e^{2x}\int_x^l \frac{q_o(\xi)}{\overline{q}} e^{-2\xi}\, d\xi - 4\frac{q_o(x)}{\overline{q}}$$

$$+ t_{r,i}^4 \frac{d^2F(x)}{dx^2} + t_{r,e}^4 \frac{d^2F(l-x)}{dx^2} = \frac{1}{\overline{q}}\frac{d^2q_o(x)}{dx^2} + H\left(\frac{d^2t_w}{dx^2} - \frac{d^2t_g}{dx^2}\right) \tag{12}$$

Equation (11) is subtracted from this equation four times to remove the integrals and give

$$\frac{1}{\overline{q}}\left(\frac{d^2q}{dx^2} - 4q\right) + t_{r,i}^4\left[\frac{d^2F(x)}{dx^2} - 4F(x)\right] + t_{r,e}^4\left[\frac{d^2F(l-x)}{dx^2} - 4F(l-x)\right]$$

$$= \frac{1}{\overline{q}}\frac{d^2q_o}{dx^2} + H\left(\frac{d^2t_w}{dx^2} - 4t_w - \frac{d^2t_g}{dx^2} + 4t_g\right) \tag{13}$$

The quantity q_o is then eliminated by differentiating equation (9a) twice and substituting into equation (13):

$$\frac{1}{\overline{q}}\left(\frac{1}{\epsilon}\frac{d^2q}{dx^2} - 4q\right) + t_{r,i}^4\left[\frac{d^2F(x)}{dx^2} - 4F(x)\right] + t_{r,e}^4\left[\frac{d^2F(l-x)}{dx^2} - 4F(l-x)\right]$$

$$= 12t_w^2\left(\frac{dt_w}{dx}\right)^2 + 4t_w^3\frac{d^2t_w}{dx^2} + H\left(\frac{1}{\epsilon}\frac{d^2t_w}{dx^2} - \frac{1}{\epsilon}\frac{d^2t_g}{dx^2} - 4t_w + 4t_g\right) \tag{14}$$

This is further simplified by eliminating d^2t_g/dx^2. Thus, equation (7a) is differentiated to give

$$\frac{d^2t_g}{dx^2} = St\left(\frac{dt_w}{dx} - \frac{dt_g}{dx}\right)$$

and equation (7a) is substituted into this to remove dt_g/dx:

$$\frac{d^2t_g}{dx^2} = St\left[\frac{dt_w}{dx} - St(t_w - t_g)\right] \tag{15}$$

Equation (15) is used to eliminate the second derivative of t_g in equation (14) with the result:

$$\frac{1}{\bar{q}}\left(\frac{l}{\epsilon}\frac{d^2q}{dx^2} - 4q\right) + t_{r,i}^4\left[\frac{d^2F(x)}{dx^2} - 4F(x)\right]$$

$$+ t_{r,e}^4\left[\frac{d^2F(l - x)}{dx^2} - 4F(l - x)\right] = 12t_w^2\left(\frac{dt_w}{dx}\right)^2 + 4t_w^3\frac{d^2t_w}{dx^2}$$

$$+ H\left\{\frac{l}{\epsilon}\frac{d^2t_w}{dx^2} - \frac{St}{\epsilon}\left[\frac{dt_w}{dx} - St(t_w - t_g)\right] - 4t_w + 4t_g\right\} \tag{16}$$

Equations (16) and (7a) are a set of two simultaneous nonlinear ordinary differential equations for t_w and t_g. Before solving them numerically, an additional simplification can be made by using an approximation for F similar to the one that was made for K. It is shown in reference 5 that $F(x)$ could be approximated quite well by the function

$$F(x) \cong \frac{e^{-2x}}{2} \tag{17}$$

By using this function, the quantity $\left(\frac{d^2F}{dx^2} - 4F\right) = 0$, and equation (16) can be rearranged into the final form:

$$\frac{d^2t_w}{dx^2}\left(4\epsilon t_w^3 + H\right) + 12\epsilon t_w^2\left(\frac{dt_w}{dx}\right)^2 - StH\,\frac{dt_w}{dx} + t_wH\left[(St)^2 - 4\epsilon\right]$$

$$= t_gH\left[(St)^2 - 4\epsilon\right] + \frac{1}{\bar{q}}\left(\frac{d^2q}{dx^2} - 4\epsilon q\right) \qquad (18)$$

Boundary conditions. - Equations (7a) and (18) are to be solved simultaneously for $t_g(x)$ and $t_w(x)$. For a first-order equation such as equation (7a) one boundary condition is required - the specified gas temperature entering the tube at $x = 0$. This gas temperature $t_g(0)$ is designated by $t_{g,i}$.

For the second-order equation (18) the boundary conditions are derived from the integral equation since the integral equation has the boundary conditions already contained within it. One of the two conditions required is found by evaluating the integral equation (11) at $x = l$ and using equation (17) to approximate F:

$$\frac{q(l)}{\bar{q}} + \frac{1}{e^{2l}}\int_0^l \frac{q_o(\xi)}{\bar{q}}\,e^{2\xi}\,d\xi + t_{r,i}^4\,\frac{e^{-2l}}{2}$$

$$+ \frac{t_{r,e}^4}{2} = \frac{q_o(l)}{\bar{q}} + H\left[t_w(l) - t_g(l)\right] \qquad (19)$$

The outgoing radiation q_o is eliminated by substituting equation (9a), and the result is rearranged into the form

$$H\left[t_w(l) - t_g(l)\right] + \epsilon t_w^4(l) - \frac{\epsilon t_{r,e}^4}{2}$$

$$- \int_0^l \left[\epsilon t_w^4 + (1 - \epsilon)H(t_w - t_g)\right]e^{-2(l-x)}\,dx = \frac{q(l)}{\bar{q}}$$

$$+ \epsilon t_{r,i}^4\,\frac{e^{-2l}}{2} - (1 - \epsilon)\int_0^l \frac{q(x)}{\bar{q}}\,e^{-2(l-x)}\,dx \qquad (20)$$

The second boundary condition for equation (18) is found by evaluating the integral equation (11) at $x = 0$ and using equation (17) to approximate F:

$$\frac{q(0)}{\bar{q}} + \int_0^l \frac{q_o(\xi)}{\bar{q}} e^{-2\xi}\, d\xi + \frac{t_{r,i}^4}{2} + t_{r,e}^4 \frac{e^{-2l}}{2} = \frac{q_o(0)}{\bar{q}} + H\left[t_w(0) - t_g(0)\right] \tag{21}$$

To begin a numerical integration of equation (18), two initial conditions are needed - t_w and dt_w/dx at $x = 0$. For each trial solution a value for t_w will be guessed. This guess temporarily takes the place of the boundary condition given by equation (20), which can only be tested after a solution has been found. The value for $dt_w/dx|_{x=0}$ will be obtained by use of the condition given by equation (21). To do this the exponential approximation (eq. (17)) for F is inserted into equation (11) which is then differentiated once and evaluated at $x = 0$:

$$\frac{1}{\bar{q}} \left.\frac{dq}{dx}\right|_0 + 2\int_0^l \frac{q_o(\xi)}{\bar{q}} e^{-2\xi}\, d\xi - t_{r,i}^4 + t_{r,e}^4 e^{-2l} = \frac{1}{\bar{q}} \left.\frac{dq_o}{dx}\right|_0 + H\left(\left.\frac{dt_w}{dx}\right|_0 - \left.\frac{dt_g}{dx}\right|_0\right) \tag{22}$$

The integral in this relation is eliminated by using the boundary condition in equation (21) to give

$$\frac{1}{\bar{q}}\left[\left.\frac{dq}{dx}\right|_0 - 2q(0)\right] - \frac{1}{\bar{q}}\left[\left.\frac{dq_o}{dx}\right|_0 - 2q_o(0)\right] - 2t_{r,i}^4 = H\left[\left.\frac{dt_w}{dx}\right|_0 - 2t_w(0) - \left.\frac{dt_g}{dx}\right|_0 + 2t_g(0)\right] \tag{23}$$

The quantities $q_o(0)$ and $\left.\frac{dq_o}{dx}\right|_0$ are eliminated by using equation (9a) and its first derivative; the derivative $\left.\frac{dt_g}{dx}\right|_0$ is eliminated by using

equation (7a). The result can then be arranged into the final form for the initial wall temperature derivative:

$$\left.\frac{dt_w}{dx}\right|_0 = \frac{1}{4\epsilon t_w^3(0) + H}\left\{H(St + 2)\left[t_w(0) - t_g(0)\right] + 2\epsilon\left[t_w^4(0) - t_{r,i}^4\right] + \frac{1}{\bar{q}}\left[\left.\frac{dq}{dx}\right|_0 - 2q(0)\right]\right\} \qquad (24)$$

This condition along with a guessed value for $t_w(0)$, a specified $t_g(0)$, heat flux distribution, and other parameters provides sufficient conditions to numerically integrate equations (18) and (7a) simultaneously. The results for each trial $t_w(0)$ are tested in the boundary condition (eq. (20)); and, if this is not satisfied, a new value for $t_w(0)$ is interpolated. The details of the numerical solution procedure for this type of simultaneous system are discussed in reference 3.

Overall Heat Balance

In addition to having each solution satisfy the required boundary conditions, a check on the numerical work was made by determining whether the solution was consistent with an overall heat balance. The heat balance was derived from the following terms:

(1) The heat removed from the tube by the heated gas, which is

$$\bar{u}\rho c_p \frac{\pi D^2}{4}\left(T_{g,e} - T_{g,i}\right)$$

(2) The radiated heat leaving the tube wall that is removed through the ends of the tube, which is

$$\pi D \int_0^L q_o\left[F\left(\frac{X}{D}\right) + F\left(\frac{L - X}{D}\right)\right]dX$$

(3) The heat gained by radiation into the tube from the environment at the ends, which is

$$\pi D\sigma\left[T_{r,i}^4 \int_0^L F\left(\frac{X}{D}\right)dX + T_{r,e}^4 \int_0^L F\left(\frac{L - X}{D}\right)dX\right]$$

(4) The heat flux supplied at the tube wall, which is $\overline{q}\pi DL$

The energy leaving the tube is equated to the incoming quantities, and the result is placed in dimensionless form:

$$\frac{H}{St}\left(t_{g,e} - t_{g,i}\right) + \int_0^l \frac{q_o}{\overline{q}}\left[F(x) + F(l - x)\right]dx$$

$$= t_{r,i}^4 \int_0^l F(x)dx + t_{r,e}^4 \int_0^l F(l - x)dx + l$$

The approximate expression for F (eq. (17)) is substituted, and the two integrals on the right are carried out. Then q_o is substituted from equation (9a), and the heat balance is arranged into the final form:

$$\epsilon l + \epsilon \frac{H}{St} t_{g,i} + \epsilon t_{r,i}^4 \frac{(1 - e^{-2l})}{4}$$

$$+ \frac{(1 - \epsilon)}{2\overline{q}} \int_0^l q(x)\left[e^{-2x} + e^{-2(l-x)}\right]dx = -\epsilon t_{r,e}^4 \frac{(1 - e^{-2l})}{4}$$

$$+ \epsilon \frac{H}{St} t_{g,e} + \frac{1}{2} \int_0^l \left[\epsilon t_w^4 + (1 - \epsilon)H(t_w - t_g)\right]\left[e^{-2x} + e^{-2(l-x)}\right]dx$$

(25)

Limiting Cases for Radiation or Convection Alone

In this section the two special cases are considered where either convection or radiation becomes very small.

Pure-radiation solution. - When convection is negligible, the pure-radiation solution can be found by following the procedure given in reference 5 where the case for uniform heating was treated. From equation (8a) when $H \to 0$ the integral equation for q_o is

$$\frac{q_o(x)}{\bar{q}} = t_{r,i}^4 F(x) + t_{r,e}^4 F(l - x) + \frac{q(x)}{\bar{q}} + \int_0^l \frac{q_o(\xi)}{\bar{q}} K(|x - \xi|)d\xi \tag{26}$$

After q_o is found, the wall temperature is obtained from equation (9a) with $H = 0$:

$$t_w^4 = \frac{q_o}{\bar{q}} + \frac{1 - \epsilon}{\epsilon} \frac{q(x)}{\bar{q}} \tag{27}$$

From this relation it is noted by considering the black wall case ($\epsilon = 1$) that $q_o/\bar{q} = t_w^4\Big|_{\epsilon=1}$; that is, $q_o/\bar{q}$ is equivalent to the black wall temperature distribution. As shown in reference 5, the general solution of equation (26) can be found by adding two more elementary solutions having the following conditions: (1) Specified reservoir temperatures with zero heating at the wall ($q = 0$) and (2) specified wall heating with zero reservoir temperatures. The solution for part (1) is given in reference 5 so part (2) is considered first. In equation (26) the reservoir temperatures are set equal to zero, and the exponential approximation (10) is used for K. Then the equation is differentiated twice, and the original equation is subtracted four times. This leads to the same result as equation (13) with H, $t_{r,i}$, and $t_{r,e}$ equal to zero:

$$\frac{d^2\left(\frac{q_o}{\bar{q}}\right)}{dx^2} = \frac{1}{\bar{q}}\left(\frac{d^2q}{dx^2} - 4q\right) \tag{28}$$

Equation (28) is integrated twice to give

$$\frac{q_o}{\bar{q}} = \frac{q}{\bar{q}} - \frac{4}{\bar{q}} \int\int q(x)dx\,dx + C_1x + C_2 \tag{29}$$

The constants C_1 and C_2 have to be determined from the boundary conditions obtained from the governing integral equation (11) with the reservoir temperatures and H equal to zero. Values for C_1 and C_2 will be determined later when a specific $q(x)$ is considered.

To obtain the wall temperature distribution, equation (27) is combined with the solution for part (1) taken from reference 5, which gives

$$t_w^4 = \frac{q_o}{\bar{q}} + \frac{1 - \epsilon}{\epsilon} \frac{q(x)}{\bar{q}} + t_{r,e}^4 + \frac{t_{r,i}^4 - t_{r,e}^4}{1 + l} \left(\frac{1}{2} + l - x \right) \tag{30}$$

where q_o/q is given by equation (29).

Pure-convection solution. - For pure convection, all the heat added at the wall is transferred to the gas. Hence, the mean gas temperature at any axial position can be found by integrating the wall heat flux from the entrance of the tube to that location:

$$\frac{\pi D^2}{4} \bar{u} \rho c_p \left[T_g(X) - T_{g,i} \right] = \pi D \int_0^X q(X) dX$$

The heat flux $q(X)$ is substituted from equation (1a), and the result can be arranged in the dimensionless form for $t_g(x)$:

$$t_g(x) = t_{g,i} + \frac{St}{H} \int_0^x \frac{q(x)}{\bar{q}} dx \tag{31}$$

From the definition of the convective heat-transfer coefficient,

$$q(X) = h \left[T_w(X) - T_g(X) \right]$$

which can be arranged in the dimensionless form

$$t_w(x) = t_g(x) + \frac{1}{H} \frac{q(x)}{\bar{q}} \tag{32}$$

Substituting $t_g(x)$ from equation (31) gives the desired wall temperature expression:

$$t_w(x) = t_{g,i} + \frac{1}{H\bar{q}} \left[q(x) + St \int_0^x q(x) dx \right] \tag{33}$$

APPLICATION TO CHOPPED SINUSOIDAL HEAT FLUX

For the numerical examples carried out herein the heat flux is assumed to have a chopped sinusoidal distribution that is often found in nuclear-reactor applications. In this case,

$$q(x) = C \sin\left[\frac{\pi(x + \delta)}{l + 2\delta}\right] \tag{34a}$$

where C is a constant. The integrated average q is given by

$$\overline{q} = C \frac{l + 2\delta}{l\pi}\left\{\cos\left(\frac{\pi\delta}{l + 2\delta}\right) - \cos\left[\frac{\pi(l + \delta)}{l + 2\delta}\right]\right\} \tag{34b}$$

This can be substituted without difficulty into equation (18) and its associated boundary conditions governing the combined radiation and convection problem.

For pure convection the solution given by equation (33) becomes

$$t_w(x) = t_{g,i} + \frac{C}{H\overline{q}}\left\{\sin\frac{\pi(x + \delta)}{l + 2\delta} + \mathrm{St}\,\frac{(l + 2\delta)}{\pi}\left[\cos\frac{\pi\delta}{l + 2\delta} - \cos\frac{\pi(x + \delta)}{l + 2\delta}\right]\right\} \tag{35}$$

For the pure-radiation solution the constants C_1 and C_2 in equation (29) are to be evaluated. Since the imposed wall heat flux is symmetric about $l/2$ and the reservoirs are both zero for the solution in equation (29), this solution must be symmetric about $l/2$; hence, $C_1 = 0$. To determine C_2 use the boundary condition found by evaluating the integral equation (11) at $x = 0$ with H, $t_{r,i}$, and $t_{r,e}$ equal to zero:

$$\frac{q(0)}{\overline{q}} + \int_0^l \frac{q_o(\xi)}{\overline{q}} e^{-2\xi}\, d\xi = \frac{q_o(0)}{\overline{q}} \tag{36}$$

When $f(x)$ is substituted into equation (29) and the integration is carried out,

$$\frac{q_o}{\overline{q}} = \frac{C}{\overline{q}}\left[1 + 4\left(\frac{l + 2\delta}{\pi}\right)^2\right] \sin\frac{\pi(x + \delta)}{l + 2\delta} + C_2 \tag{37}$$

This is substituted into equation (36), and after integrating the result can be solved for the constant C_2. This constant is inserted back into equation (37) to obtain $q_o/\overline{q}$, which is then substituted into equation (30) to obtain the final wall temperature distribution for pure radiation:

$$t_w^4 = t_{r,e}^4 + \frac{t_{r,i}^4 - t_{r,e}^4}{l + l}\left(\frac{l}{2} + l - x\right) + \frac{C}{\overline{q}}\left\{\left[\frac{1}{\epsilon} + \frac{4(l + 2\delta)^2}{\pi^2}\right]\sin\frac{\pi(x + \delta)}{l + 2\delta}\right.$$

$$+ \frac{2(l + 2\delta)}{(e^{-2l} + 1)\pi}\left[\cos\frac{\pi\delta}{l + 2\delta} - e^{-2l}\cos\frac{\pi(l + \delta)}{l + 2\delta}\right.$$

$$\left.\left. - \frac{2(l + 2\delta)}{\pi}\left(\sin\frac{\pi\delta}{l + 2\delta} + e^{-2l}\sin\frac{\pi(l + \delta)}{l + 2\delta}\right)\right]\right\}$$

DIMENSIONLESS PARAMETERS

Before presenting some numerical examples, it is worthwhile to discuss the independent parameters that are involved and become familiar with their range of numerical magnitudes:

(1) The parameter l is the length-diameter ratio of the tube. Cases are carried out in the range from $l = 5$ to 100. Most of the results are given for $l = 50$.

(2) The emissivity ϵ of the internal tube surface varies in the range from 1.0 for the black condition to 0.01, which is a lower limit for some highly polished metals. In previous work (ref. 3) most of the results were found to be fairly insensitive to ϵ; and, hence, except for one example, the present solutions are carried out for the black condition.

(3) Three of the parameters are dimensionless temperatures: $t_{g,i}$, $t_{r,i}$, and $t_{r,e}$. The dimensionless temperature variable is defined as $T(\sigma/\overline{q})^{1/4}$ and thus depends not only on T but on the average wall heat flux. Some typical values are:

$\overline{q}$, Btu/(hr)(sq ft)	T, $^{\circ}$R	t, dimensionless
50,000	2000	0.86
100,000	3000	1.09
100,000	5000	1.81

(4) The parameter St is the Stanton number $4h/\overline{u}\rho c_p = 4Nu/RePr$. For turbulent flow in a tube a commonly known correlation is $Nu = 0.023\ Re^{0.8}Pr^{0.4}$ so that $St = 0.092\ Re^{-0.2}Pr^{-0.6}$. For gases at elevated temperatures let $Pr = 0.75$ so $St = 0.109/Re^{0.2}$. Then some values are:

Re	St
10^4	0.0173
10^5	.0109
10^6	.00685

(5) The dimensionless heat-transfer coefficient is given by $\frac{h}{\overline{q}}\left(\frac{\overline{q}}{\sigma}\right)^{1/4}$. Some typical values are:

h, Btu/(hr)(sq ft)($^\circ$R)	$\overline{q}$, Btu/(hr)(sq ft)	H, dimensionless
10	10^5	0.28
40	10^5	1.10
50	2×10^5	.82

(6) The chopped sine wall heat flux has the form $\sin\frac{\pi(x+\delta)}{l+2\delta}$, which contains the parameter δ that can vary from zero to ∞. Practical values for nuclear reactors are in a range from about 0 to $l/4$. The maximum variation in $q(x)$ is when $\delta = 0$ and will be the case considered here. Results for other δ will lie between those in the present report and those in reference 3 where q was uniform along the tube ($\delta \to \infty$).

DISCUSSION

With several independent parameters to consider, it is not feasible to examine the wide variety of types of solutions in any detail. Several typical examples are considered that will indicate the general behavior of the wall and gas temperatures. For some ranges of parameters the combined radiation and convection solutions (these solutions will be referred to as simply the combined solutions) become very close to the results for radiation or convection alone; hence, when these ranges are defined, the solutions falling within them are easily determined from the limiting cases.

The first parameter to be discussed is the effect of tube length. This is shown in figure 2 where dimensionless wall and gas temperature distributions are given for black tubes with various lengths from 5 to 100 diameters. The wall heat flux has a one-half sine wave variation; that is, the parameter δ is zero. Three groups of wall temperature curves are given: The solid curves are the combined convection and radiation solutions, the dotted curves are for convection alone, and the dot-dash lines are for radiation alone. Typical values for St, H, and $t_{g,i}$ have been chosen. The reservoirs at the inlet and exit ends of the tube have been assumed equal, respectively, to the inlet and exit gas temperatures. As the limiting case of pure radiation is approached, the convective heat transfer becomes very small and a negligible quantity of heat is transferred to the gas so that $t_{g,e} = t_{g,i}$. Hence, for the pure radiation solutions, both the exit and inlet reservoir temperatures are set equal to $t_{g,i}$.

Consider first the three curves for a short tube, $l = 5$. The pure-convection curve is generally much higher than the pure-radiation curve, indicating that the wall heat flux can be dissipated more easily by radiation to the cooler end reservoirs than by convection to the gas. Since the radiation process is more efficient, the combined solution follows the shape of the radiative distribution and is somewhat below the radiation curve because of the additive convective effect. Since q is zero at $x = 0$, it follows from the relation $q = h(T_w - T_g)$ that the pure-convection curves begin at $t_{g,i}$. The combined solutions begin at values higher than $t_{g,i}$ because radiation from the central part of the tube imposes an additional heat load on the wall near the tube inlet.

For a long duct ($l = 100$) the situation is completely different. Here the pure-radiation process leads to very high wall temperatures as it is difficult for heat to be radiated from the central region of a long tube to the end reservoirs. The energy can be carried away much more easily by the flowing gas, and as a result the wall temperatures for the combined solutions are close to the pure-convection curve. For tubes longer than 100 diameters, and for the parameters in figure 2, the combined solutions would be so close to the pure-convection limit that this limit would serve as an adequate approximation.

The lower part of figure 2 shows the variation of gas temperature along the tube as compared with the pure convective case. With a sinusoidal heat flux variation along the tube, the gas temperature rises slowly at first and then at a more rapid rate in the central part of the tube where the heat addition reaches a maximum. For long tubes the gas temperature begins to rise a little more rapidly than for the pure-convection result because of the additional heat radiated to the wall near the inlet. For short tubes the exit gas temperature is considerably below the pure-convection value because of radiation losses to the inlet

and exit reservoirs. It is important to note that, although the maximum wall temperatures have been reduced compared with pure convection, the exit gas temperatures have also been reduced. For a length of 50 diameters the peak temperature is decreased by 7 percent while the exit gas temperature has been reduced by 4 percent. Thus, if the heat flux were raised to yield the same exit gas temperature, the wall temperatures would rise somewhat, and the reduction in the maximum values would only be about 5 percent.

Figure 2 has been restricted to black tubes, and the question arises as to how the wall emissivity will influence the results. This report is mainly interested in long tubes because of their greater practical use. In this case the solutions are strongly dominated by convection and in most instances are fairly close to the convection curves. Reducing the emissivity of the surface would be expected to decrease the radiation exchanges and hence move the solutions toward the convection curves. As a result, for emissivities less than 1, the combined solutions should fall between the black curve and the pure-convection case. This is illustrated in figure 3 for a tube 20 diameters long. Even for a very small ϵ of 0.01 it is found that the solution is still close to the black curve. This is due to the multiple reflections inside the tube that tend to make the tube act like a black enclosure. Due to this insensitivity with ϵ and the fact that all the curves for long tubes will lie in the relatively narrow range between the black and pure-convection results, solutions are given on the remaining figures only for the black case. Additional information on the influence of ϵ can be obtained by looking at the results for uniform heating in reference 3.

Figure 4 illustrates the effect of changing the Stanton number. For turbulent flow St is proportional to $1/Re^{0.2}$ so an increase in St is caused by a decrease in Reynolds number, which in turn would be caused by a decreased mass-flow rate. This increases the temperature rise of the gas as it remains in the tube a longer time, and consequently the wall temperatures are increased when St is made larger. This causes larger radiation losses so that the exit gas temperature ratio is decreased as shown in the lower part of the figure. For St smaller than 0.01, radiation effects are reduced, and the solutions would approach the pure-convection limit more closely.

Figure 5 illustrates the influence of the dimensionless heat-transfer coefficient H. When H = 0.8, the wall temperatures for convection alone are much lower than the pure-radiation curve, indicating that the imposed wall heat flux can be removed much more easily by convection. Consequently, the solution is close to the pure-convection curve. As H is decreased, the convection becomes less effective, and the solutions move toward the pure-radiation result. For H = 0.2, the solution is strongly radiation dominated, and large quantities of energy

are lost from the ends of the tube as evidenced by the lower exit gas temperature. For H greater than 0.8, the solutions could be predicted quite well from the pure-convection case.

When the inlet gas temperature is changed, the temperature level of the entire tube is altered. For low inlet temperatures the radiation effects are suppressed; and, as shown in figure 6, when $t_{g,i} = 0.5$, the solution is close to the pure-convection result. For lower values of $t_{g,i}$ radiation exchange can be neglected. When $t_{g,i} = 3.0$, however, radiation is appreciable and causes the wall temperature curve to be more uniform than for convection alone.

In some applications the ends of the tube will be exposed to environment temperatures other than the inlet or exit gas temperatures. For example, a tube could be exhausting to the very low temperature of outer space, or one end of the tube could be exposed to a high temperature such as a combustion chamber. A few of these effects are illustrated in figure 7. Figure 7(a) shows the effect of having an elevated reservoir temperature at the exit end of the tube. The wall temperatures near the exit are strongly influenced by the heat radiated into the tube, and the temperature at $x = l$ is raised close to the exit reservoir value. Figure 7(b) illustrates the result of raising both the inlet and exit reservoir temperatures so heat is now radiated into both ends of the tube. The gas temperatures in figure 7(b) are always above the pure-convection solution because of the additional heat that is radiated to the walls and then transferred to the gas. Figure 7 demonstrates the very great effect that the environment temperatures can have on the tube wall temperatures.

As indicated by the exit gas temperature, for most of the sample cases given here there were net radiation losses from the end openings of the tube. It is of interest to note how much of the imposed wall heat flux is transferred to the gas in comparison with the individual end losses. These quantities can be evaluated from the terms in the heat balance equation (25), and results are given in table I, which lists the heat radiated from each end of the tube and the heat convected to the gas, these quantities being normalized with respect to the total heat generation imposed at the tube wall. An interesting case at the bottom of table I is when the inlet reservoir is heated to $t_{r,i} = 3.0$, as in this instance the heat gain (a heat gain appears as a negative number) by the wall from incoming radiation is appreciable compared with the specified wall heating.

CONCLUDING REMARKS

An analysis has been carried out to study combined radiation and convection for transparent gas flowing in a tube with an arbitrary axial distribution of imposed wall heat flux. The results were then specialized for a sinusoidal heat flux variation, and several numerical examples were computed to illustrate the effect of the independent parameters. Most of the examples were carried out for tubes 50 diameters in length, and only a few cases are shown for shorter tubes that are not as important practically. The internal radiation tends to level out the wall temperature distribution in the tube because of heat being radiated axially from the hot to cooler regions. If the outside environment temperature is high, large quantities of heat can be radiated into the tube and cause large local increases in wall temperature.

There are a few final remarks that should be made with reference to the analytical procedure. One of the most important assumptions was the use of the separable kernel method which made it possible to convert the governing integral equation into a differential equation. This method was used previously in a paper dealing with specular reflections in a uniformly heated tube (ref. 7) where it is compared with direct numerical solutions of the integral equation. For tubes 20 diameters in length the separable kernel gave wall temperatures about 5 percent too high, whereas for short ducts the error was very small. This indicates that for tubes 50 diameters long the pure-radiation curves are probably about 10 percent too high. However, for long tubes convection generally becomes more dominant than radiation so an error in the radiation terms is less important. It appears that the separable kernel method will only introduce an inaccuracy of a few percent in the combined convection and radiation solutions considered herein.

Another important assumption was the use of a constant convective heat-transfer coefficient. In the thermal entrance region which, for turbulent flow, extends over approximately the first 10 diameters of the tube, the heat-transfer coefficient will be higher than in the fully developed region. This will cause a larger convection effect near the entrance of the tube than was accounted for in the analysis; and, for the first several diameters, the solutions should be closer to the pure-convection curves. Since the heat-transfer coefficient is very high at the tube entrance, the tube wall temperature at $x = 0$ would be close to the inlet gas temperature. For most of the present numerical examples this effect is not too significant because the imposed sinusoidal heating decreases to zero at the tube entrance. With only a small heat input near the tube entrance, the wall temperatures are already close to the gas temperature; and, hence, the magnitude of the heat-transfer coefficient is not as important in this region.

Lewis Research Center
National Aeronautics and Space Administration
Cleveland, Ohio, July 13, 1962

APPENDIX - SYMBOLS

A	surface area
c_p	specific heat of fluid
D	tube diameter
F	radiation configuration factor from a differential ring element on tube wall to circular opening at tube end
H	dimensionless heat-transfer coefficient, $\frac{h}{\overline{q}}\left(\frac{\overline{q}}{\sigma}\right)^{1/4}$
h	convective heat-transfer coefficient
$K\,dx$	radiation configuration factor between differential ring elements on inside of tube wall
k	thermal conductivity of gas
L	length of tube
l	dimensionless length, L/D
Nu	Nusselt number, hD/k
Pr	Prandtl number, $c_p\mu/k$
q	heat added per unit area at tube wall
$\overline{q}$	integrated average q
q_i	total incoming radiation to surface per unit area
q_o	total outgoing radiation from surface per unit area
Re	Reynolds number, $\overline{u}D\rho/\mu$
St	Stanton number, $4h/\overline{u}\rho c_p = 4Nu/RePr$
T	absolute temperature
t	dimensionless absolute temperature, $(\sigma/\overline{q})^{1/4}T$
u	gas velocity
$\overline{u}$	mean gas velocity

X axial length coordinate measured from tube entrance

x dimensionless coordinate X/D

δ linear extrapolation distance in chopped sine heat flux distribution

ϵ emissivity of surface

μ viscosity of gas

Ξ length coordinate

ξ dimensionless length, Ξ/D

ρ density of gas (except in eq. (6) where ρ is reflectivity)

σ Stefan-Boltzmann constant

Subscripts:

e exit of tube

g gas

i inlet of tube (except in q_i)

r reservoir or environment at end of tube

w internal surface of tube wall

REFERENCES

1. Hottel, H. C.: Geometrical Problems in Radiant Heat Transfer. Heat Transfer Lectures, vol. II. NEPA-979 IER-13, Fairchild Engine and Airplane Corp., June 1, 1949, pp. 76-95.

2. Perlmutter, M., and Siegel, R.: Heat Transfer by Combined Forced Convection and Thermal Radiation in a Heated Tube. Paper 61-WA-169, ASME, 1961. (To be publ. in Jour. Heat Transfer.)

3. Siegel, R., and Perlmutter, M.: Convective and Radiant Heat Transfer for Flow of a Transparent Gas in a Tube with a Gray Wall. Int. Jour. Heat and Mass Transfer, vol. 5, no. 5, July 1962, pp. 639-660.

4. Jakob, Max: Heat Transfer. Vol. II. John Wiley & Sons, Inc., 1957.

5. Usiskin, C. M., and Siegel, R.: Thermal Radiation from a Cylindrical Enclosure with Specified Wall Heat Flux. Jour. Heat Transfer, ser. C, vol. 82, no. 4, Nov. 1960, pp. 369-374.

6. Buckley, H.: On the Radiation from the Inside of a Circular Cylinder, pt. I. Phil. Mag., vol. 4, no. 23, Oct. 1927, pp. 753-762. (See also Phil. mag., pt. II, vol. 6, Sept. 1928, pp. 447-457.)

7. Perlmutter, M., and Siegel, R.: Effect of Specularly Reflecting Gray Surface on Thermal Radiation Through a Tube and from Its Heated Wall. Paper 62-HT-4, ASME, 1962. (To be publ. in Jour. Heat Transfer.)

TABLE I. - FRACTIONS OF HEAT TRANSFERRED BY CONVECTION AND RADIATION FOR SINUSOIDAL HEAT INPUT, $\delta = 0$

		$t_{r,e}$	$\frac{\text{Convection out}}{\text{Wall heat generation}}$	$\frac{\text{Radiation to inlet reservoir}}{\text{Wall heat generation}}$	$\frac{\text{Radiation to outlet reservoir}}{\text{Wall heat generation}}$
Effect of l $\epsilon = 1$, St = 0.01, H = 0.8, $t_{r,i} = t_{g,i} = 1.5$, $t_{r,e} = t_{g,e}$	$l = 5$ 10 20 30 50 100	1.52 = $t_{g,e}$ 1.57 = 1.70 = 1.83 = 2.10 = 2.73 = ↓	0.372 .592 .803 .890 .954 .982	0.316 .204 .094 .048 .015 .003	0.312 .204 .103 .062 .031 .015
Effect of ϵ $l = 20$, St = 0.01, H = 0.8, $t_{r,i} = t_{g,i} = 1.5$, $t_{r,e} = t_{g,e}$	$\epsilon = 1$ .01	1.70 = $t_{g,e}$ 1.71 = ↓	0.803 .834	0.094 .082	0.103 .084
Effect of St $l = 50$, $\epsilon = 1$, H = 0.8, $t_{r,i} = t_{g,i} = 1.5$, $t_{r,e} = t_{g,e}$	S = 0.01 .02	2.10 = $t_{g,e}$ 2.66 = ↓	0.954 .931	0.015 .018	0.031 .051
Effect of H $l = 50$, $\epsilon = 1$, St = 0.01, $t_{r,i} = t_{g,i} = 1.5$, $t_{r,e} = t_{g,e}$	H = 0.2 .4 .8	2.80 = $t_{g,e}$ 2.49 = 2.10 = ↓	0.518 .794 .954	0.229 .086 .015	0.253 .120 .031
Effect of $t_{g,i}$ $l = 50$, $\epsilon = 1$, St = 0.01, H = 0.8, $t_{r,i} = t_{g,i}$, $t_{r,e} = t_{g,e}$	$t_{g,i} = 0.5$ 1.5 3.0	1.12 = $t_{g,e}$ 2.10 = 3.50 = ↓	0.992 .954 .804	0 .015 .093	0.008 .031 .103
Effect of $t_{r,i}$ $l = 50$, $\epsilon = 1$, St = 0.01, H = 0.8, $t_{g,i} = 0.5$	$t_{r,i} = 0.5$ .5 3.0 3.0 3.0	3 5 2.5 3.5 5.5	1.11 1.42 1.18 1.28 1.68	0 0 [a]-.13 [a]-.13 [a]-.13	[a]-0.11 [a]-.42 [a]-.05 [a]-.15 [a]-.55

[a]Minus sign denotes net heat gain.

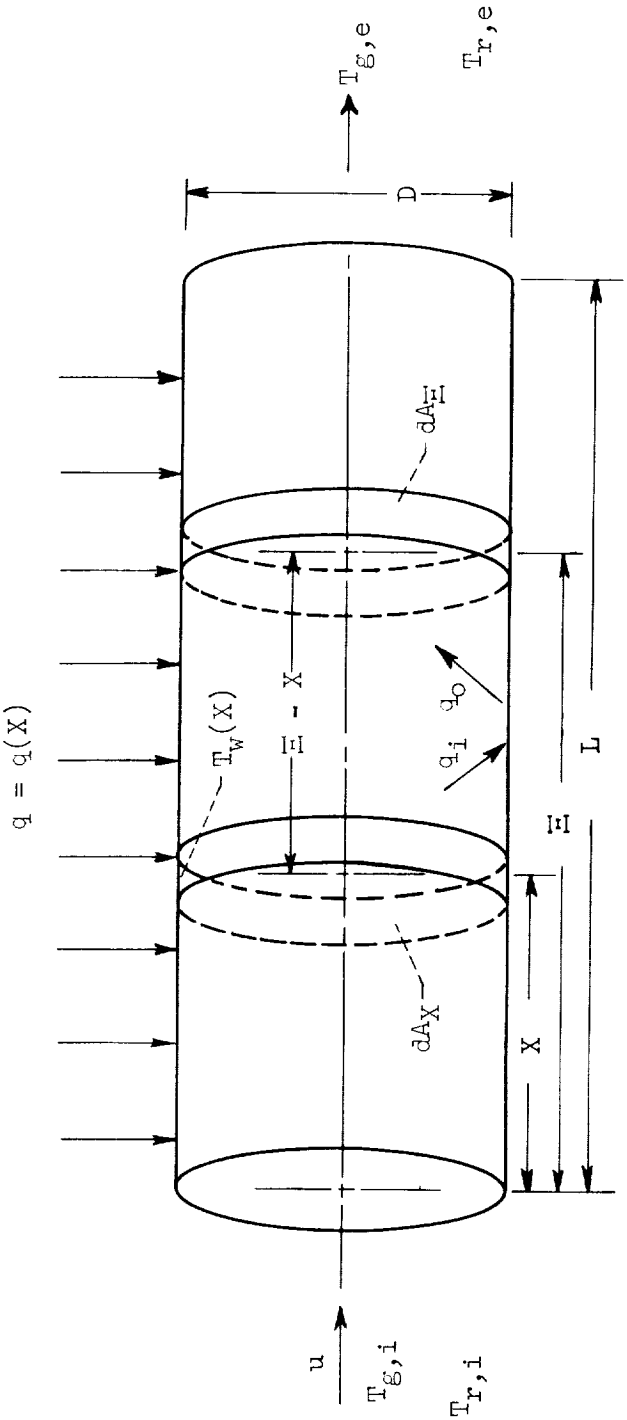

Figure 1. - Circular tube with nonuniform wall heat flux.

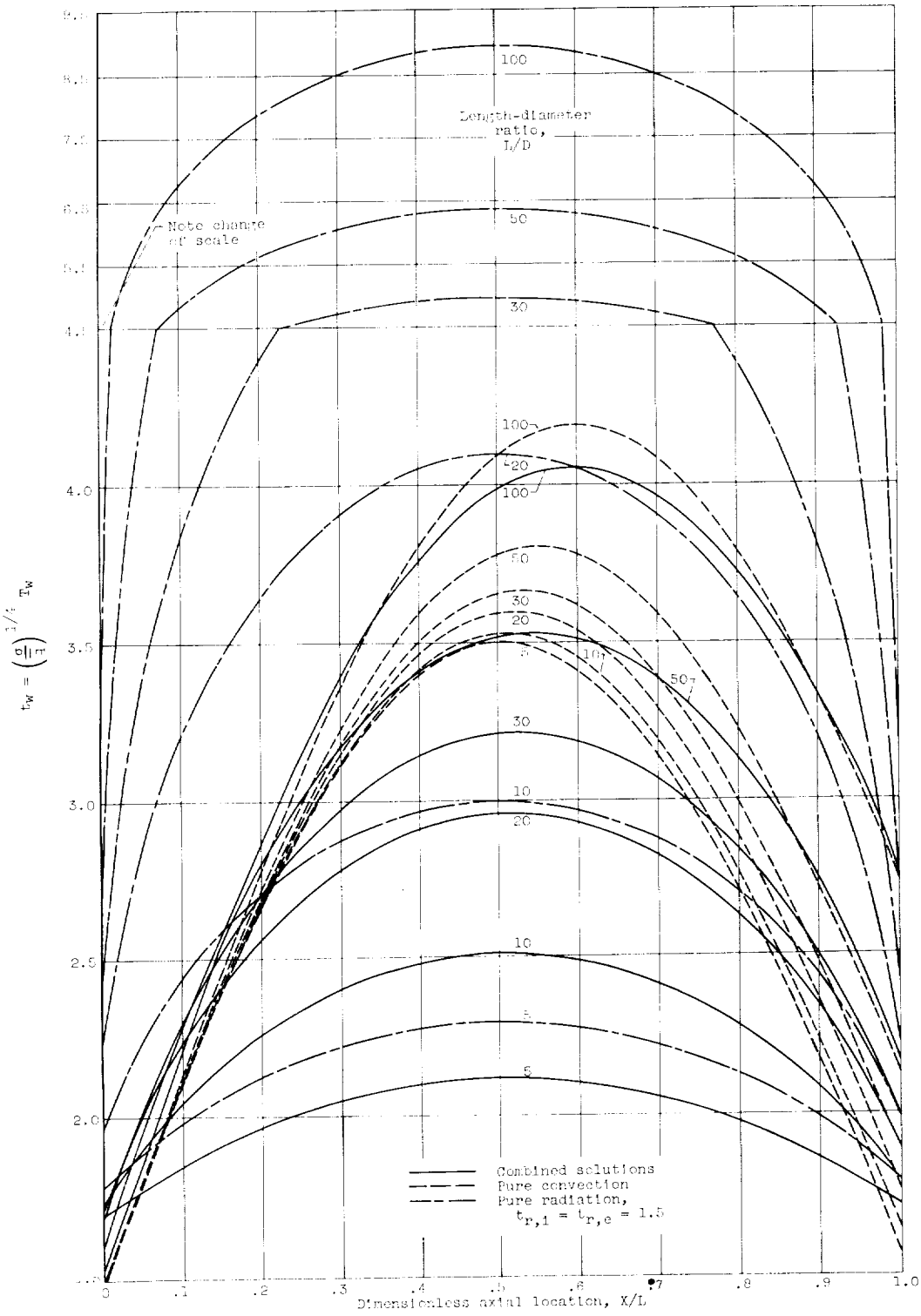

(a) Wall temperature distribution.

Figure 2. - Effect of tube length-diameter ratio on wall and gas temperature distributions. $\epsilon = 1$, St = 0.01, H = 0.8, $t_{r,i} = t_{g,i} = 1.5$, $t_{r,e} = t_{g,e}$, $\beta = 0$.

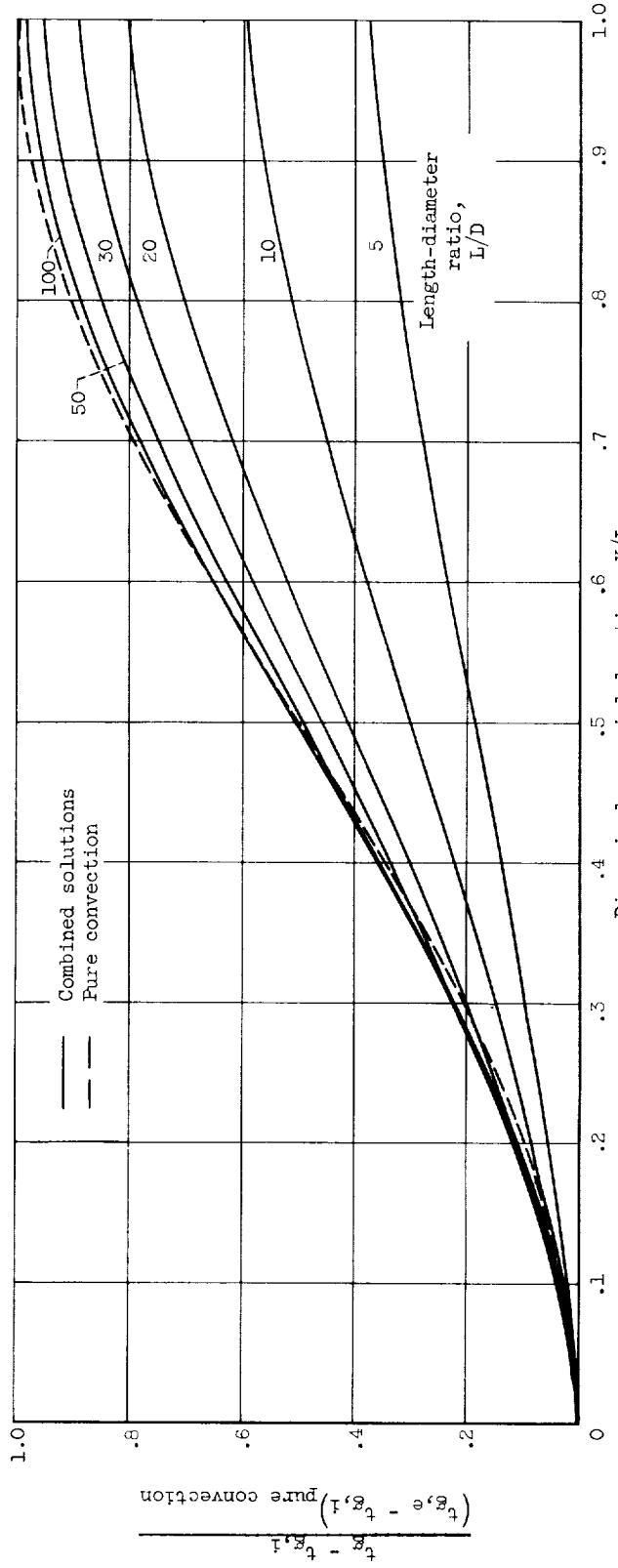

(b) Gas temperature distribution.

Figure 2. - Concluded. Effect of tube length-diameter ratio on wall and gas temperature distributions. $\epsilon = 1$, St = 0.01, H = 0.8, $t_{r,i} = t_{g,i} = 1.5$, $t_{r,e} = t_{g,e}$, $\delta = 0$.

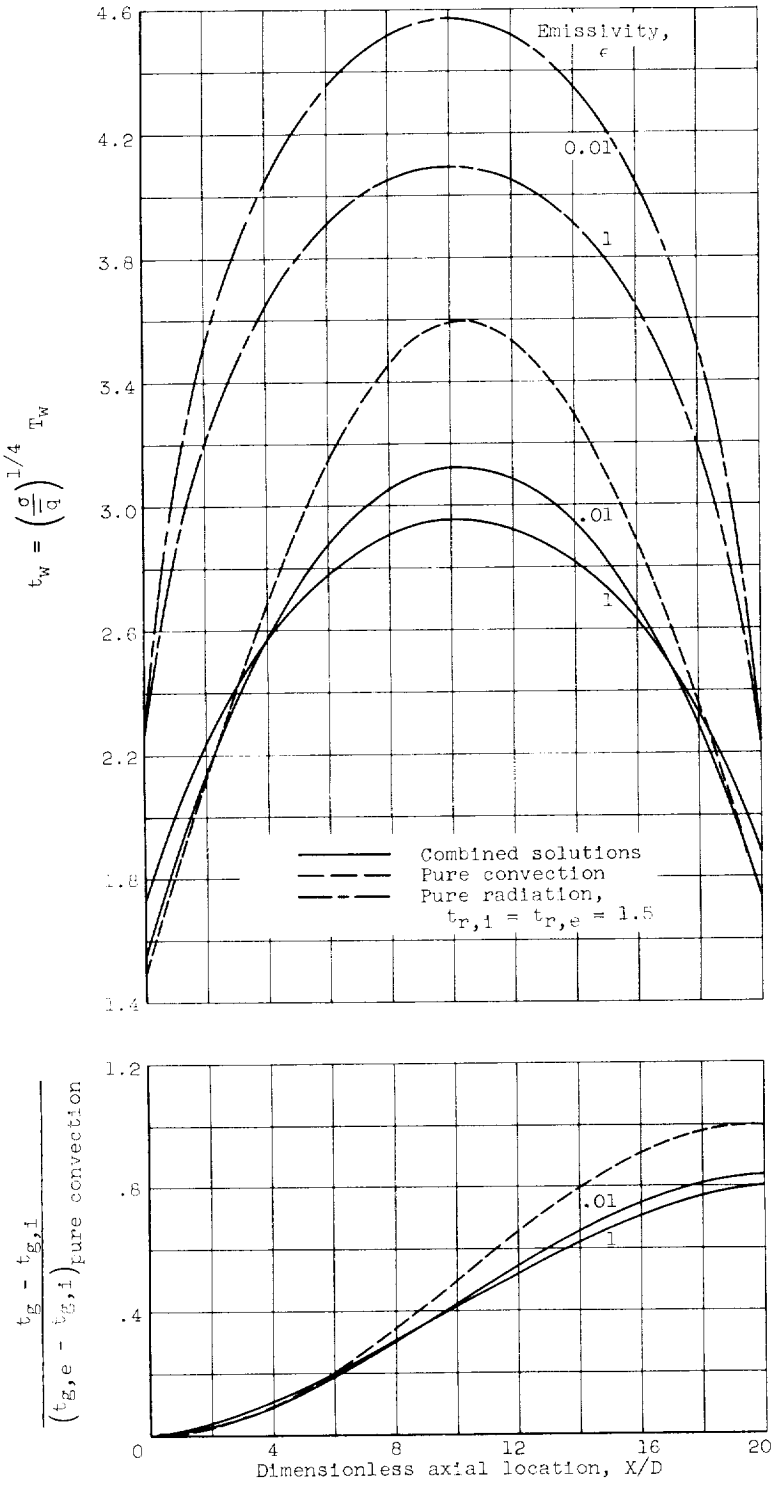

Figure 3. - Effect of emissivity on temperature distributions in a tube 20 diameters long. St = 0.01, H = 0.8, $t_{r,i} = t_{g,i} = 1.5$, $t_{r,e} = t_{g,e}$, $\delta = 0$.

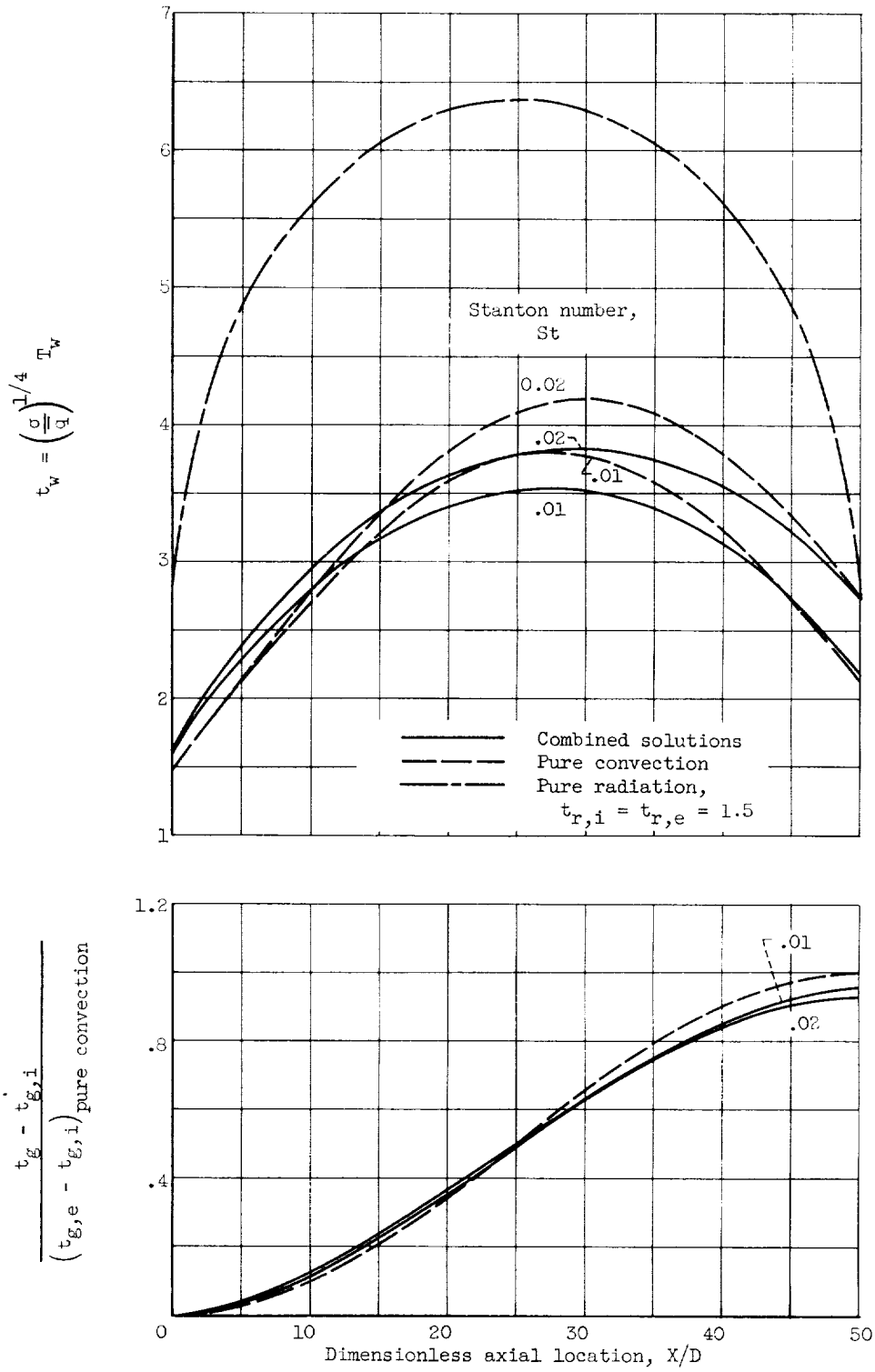

Figure 4. - Effect of Stanton number on temperature distributions in a tube 50 diameters long. $\epsilon = 1$, $H = 0.8$, $t_{r,i} = t_{g,i} = 1.5$, $t_{r,e} = t_{g,e}$, $\delta = 0$.

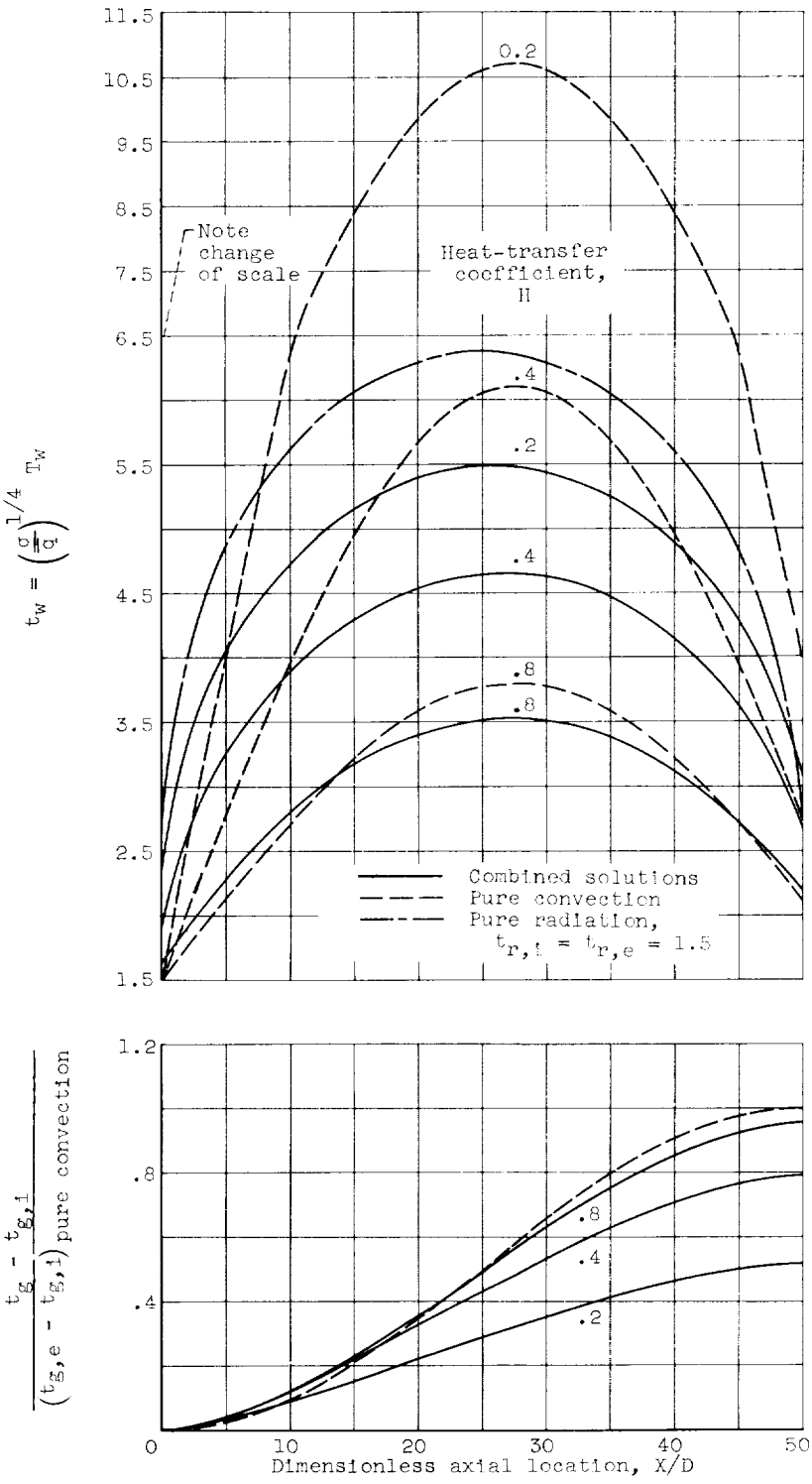

Figure 5. - Effect of dimensionless heat-transfer coefficient on temperature distributions in a tube 50 diameters long. $\epsilon = 1$, St = 0.01, $t_{r,i} = t_{g,i} = 1.5$, $t_{r,e} = t_{g,e}$, $\delta = 0$.

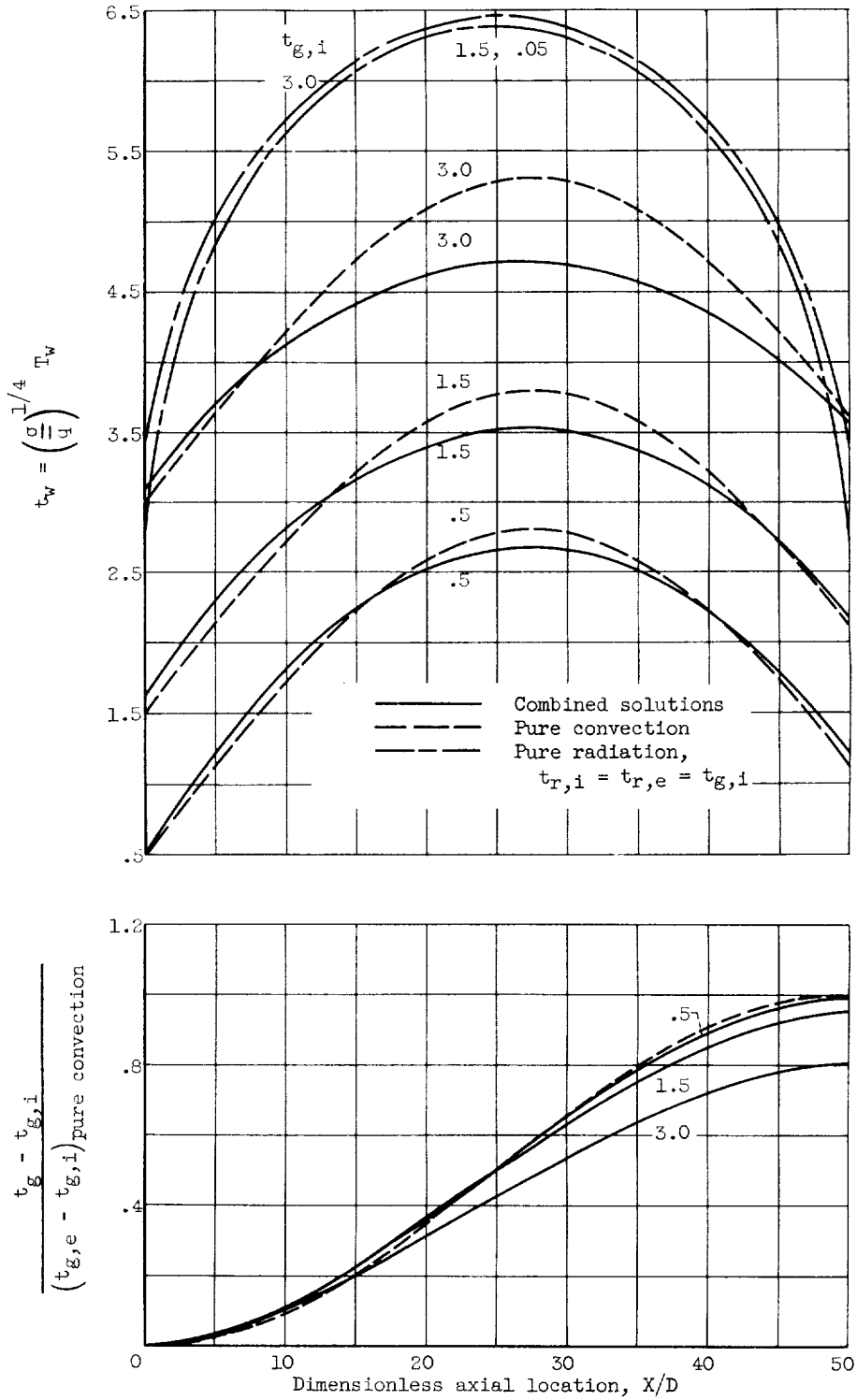

Figure 6. - Effect of inlet gas temperature on temperature distributions in a tube 50 diameters long. $\epsilon = 1$, $St = 0.01$, $H = 0.8$, $t_{r,i} = t_{g,i}$, $t_{r,e} = t_{g,e}$, $\delta = 0$.

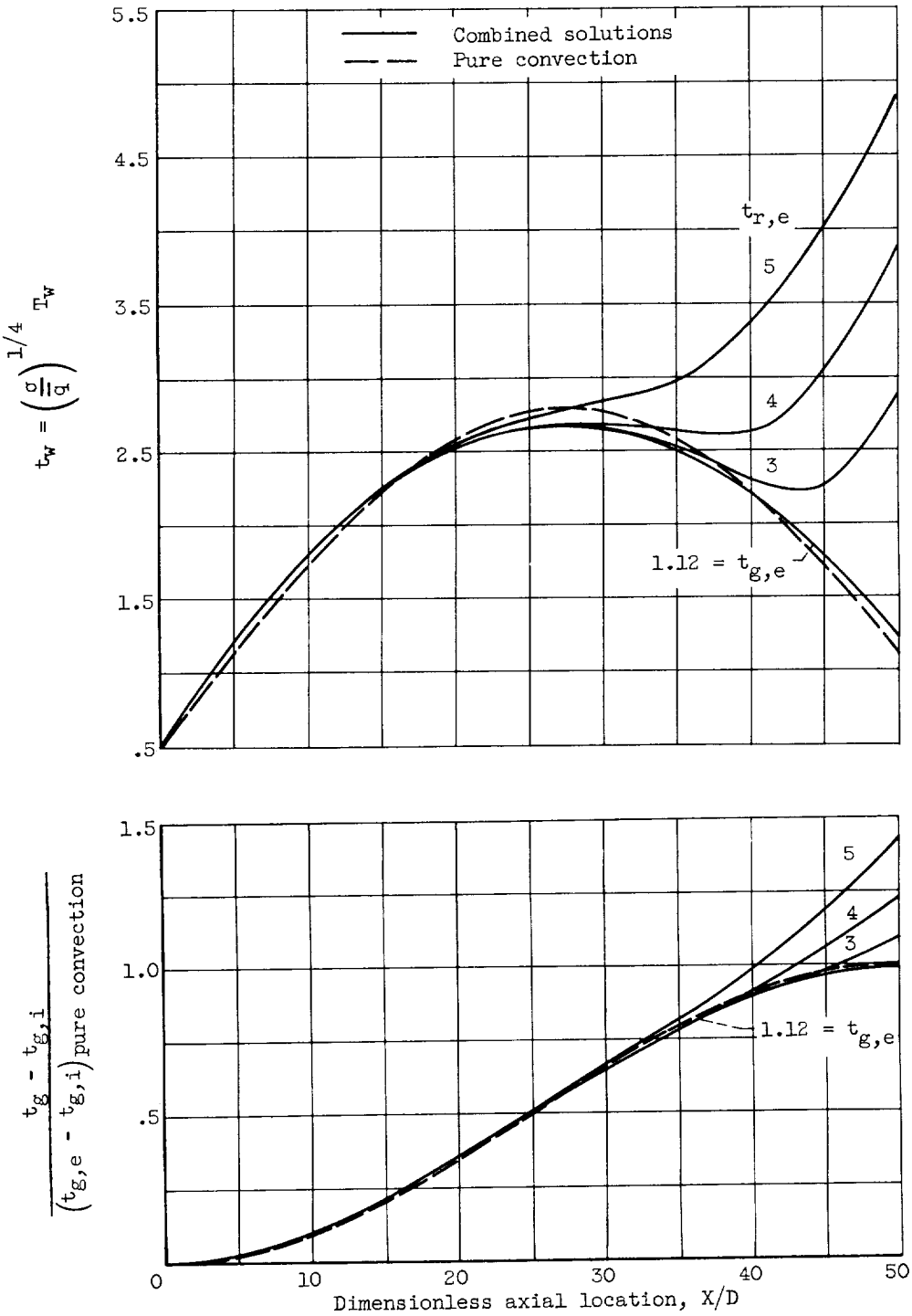

(a) $t_{r,i} = t_{g,i} = 0.5$.

Figure 7. - Effect of exit reservoir temperature on temperature distributions in a tube 50 diameters long. $\epsilon = 1$, St = 0.01, H = 0.8, $\delta = 0$.

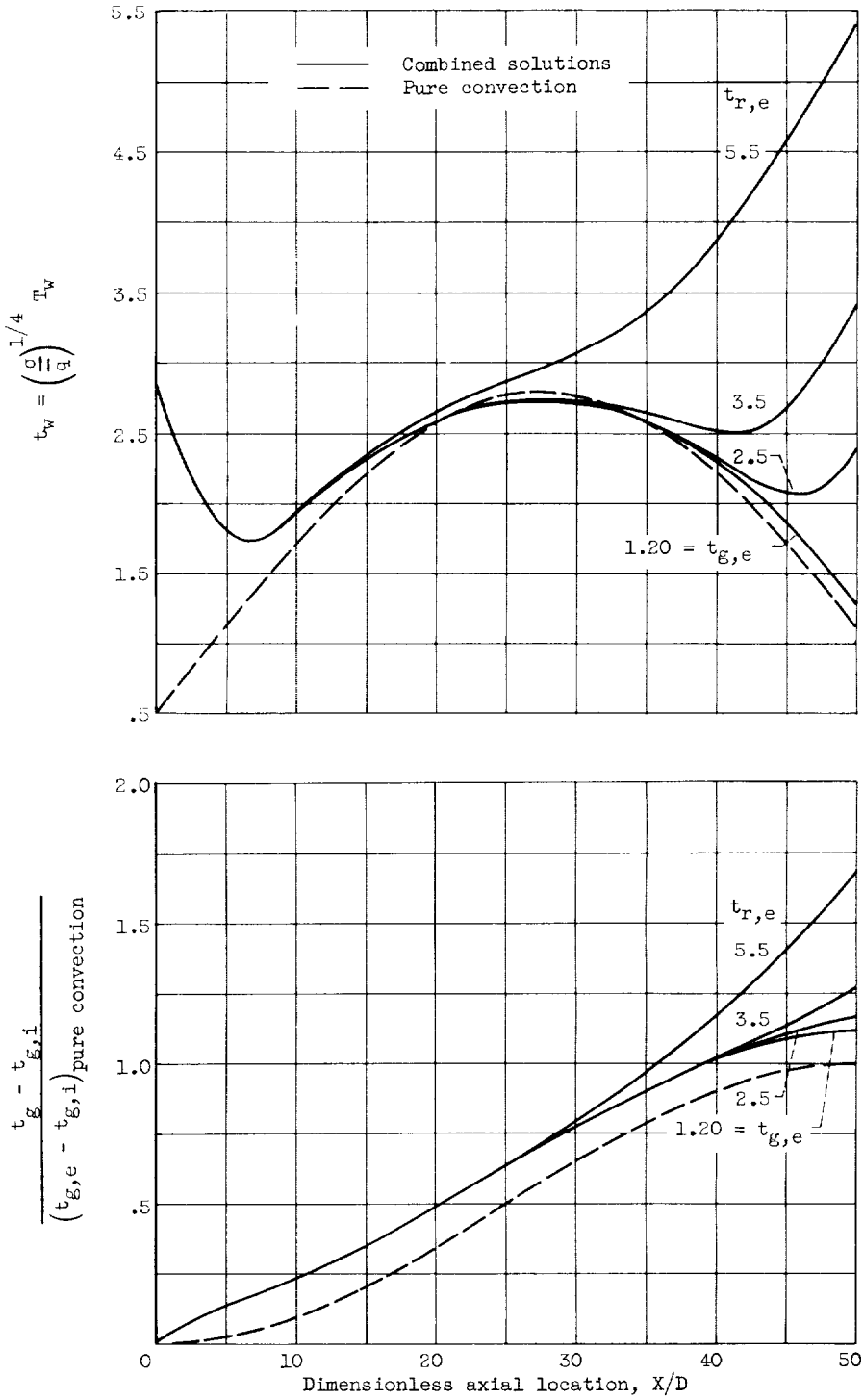

(b) $t_{r,i} = 3.0$, $t_{g,i} = 0.5$.

Figure 7. - Concluded. Effect of exit reservoir temperature on temperature distributions in a tube 50 diameters long. $\epsilon = 1$, St = 0.01, H = 0.8, $\delta = 0$.

NASA-Langley, 1962 E-1672